

行政院國家科學委員會專題研究計畫 成果報告

Flavokawain A 和 Flavokawain B 對人類乳癌細胞之體內及
體外抑制增生、腫瘤入侵作用和誘發細胞程式死亡機制之
探討

研究成果報告(精簡版)

計畫類別：個別型
計畫編號：NSC 95-2314-B-041-003-
執行期間：95年11月01日至96年07月31日
執行單位：嘉南藥理科技大學藥學系

計畫主持人：許雅玲
共同主持人：郭柏麟
計畫參與人員：碩士班研究生-兼任助理：倪雯秋



處理方式：本計畫涉及專利或其他智慧財產權，2年後可公開查詢

中華民國 96 年 10 月 15 日

行政院國家科學委員會專題研究計畫 成果報告

Flavokawain A 和 Flavokawain B 對人類乳癌細胞之體內及體外抑制增生、腫瘤入侵作用和誘發細胞程式死亡機制之探討

計畫類別：個別型計畫

計畫編號：NSC 95-2314-B-041 -003

執行期間：2006 年 8 月 01 日至 2007 年 07 月 31 日

計畫主持人：許雅玲

共同主持人：郭柏麟

計畫參與人員：倪雯秋

成果報告類型：精簡報告

處理方式：本計劃暫不公開

執行單位：嘉南藥理科技大學生物科技系

中 華 民 國 96 年 10 月 8 日

行政院國家科學委員會專題研究計畫成果報告

Flavokawain A 和 Flavokawain B 對人類乳癌細胞之體內及體外抑制

增生、腫瘤入侵作用和誘發細胞程式死亡機制之探討

計畫編號：NSC 95-2314-B-041 -003

執行期限：2006年8月01日至2007年07月31日

主持人：許雅玲，嘉南藥理科技大學生物科技系

處理方式：本計畫暫不公開



Isoobtusilactone A Induces Cell Cycle Arrest and Apoptosis through Reactive Oxygen Species/Apoptosis Signal-Regulating Kinase 1 Signaling Pathway in Human Breast Cancer Cells

Po-Lin Kuo,¹ Chung-Yi Chen,³ and Ya-Ling Hsu²

¹Cell Biology Laboratory, Department of Biotechnology, and ²Department of Pharmacy, Chia-Nan University of Pharmacy and Science, Tainan, Taiwan; and ³Basic Medical Science Education Center, Fooyin University, Kaohsiung, Taiwan

Abstract

This study is the first to investigate the anticancer effect of isoobtusilactone A (IOA) in two human breast cancer cell lines, MCF-7 and MDA-MB-231. IOA exhibited effective cell growth inhibition by inducing cancer cells to undergo G₂-M phase arrest and apoptosis. Further investigation revealed that IOA's inhibition of cell growth was also evident in a nude mice model. Cell cycle blockade was associated with increased levels of p21 and reduced amounts of cyclin B1, cyclin A, cdc2, and cdc25C. IOA also enhanced the levels of inactivated phosphorylated cdc2 and cdc25C. IOA triggered the mitochondrial apoptotic pathway, as indicated by a change in Bax/Bcl-2 ratios, resulting in mitochondrial membrane potential loss, cytochrome *c* release, and caspase-9 activation. We also found that the generation of reactive oxygen species (ROS) is a critical mediator in IOA-induced cell growth inhibition. Enhancement of ROS by IOA activated apoptosis signal-regulating kinase 1 (ASK1) resulted in the increased activation of c-Jun NH₂-terminal kinase and p38. Antioxidants EUK8 and N-acetyl cysteine significantly decreased apoptosis by inhibiting the ASK1 dephosphorylation at Ser⁹⁶⁷ and subsequently increased the interaction of ASK1 with thioredoxin or 14-3-3 proteins. Moreover, blocking ASK1 by small interfering RNA inhibition completely suppressed IOA-induced apoptosis. Taken together, these results imply a critical role for ROS and ASK1 in IOA's anticancer activity. [Cancer Res 2007;67(15):7406–20]

Introduction

Breast cancer is one of the most common malignancies in women and is the leading cause of death worldwide for women between the ages of 40 and 55 (1). This pathology is currently controlled by surgery and radiotherapy and is frequently supported by adjuvant chemo- or hormonotherapies (1, 2). However, breast cancer is highly resistant to chemotherapy, and there is still no effective cure for patients with advanced stages of the disease, especially in cases of hormone-independent cancer (2, 3). Effective chemopreventive treatment for breast cancer would have a tremendous impact on breast cancer morbidity and mortality.

Reactive oxygen species (ROS) are derived from the metabolism of molecular oxygen. ROS include superoxide anion radical (O₂⁻), singlet oxygen (¹O₂), hydrogen peroxide (H₂O₂), and the highly reactive hydroxyl radical (·OH; refs. 4, 5). ROS normally exist in

balance with biochemical antioxidants in all aerobic cells (4–7). Oxidative stress occurs when this critical balance is disrupted because of excess ROS, antioxidant depletion, or both. Evidence is accumulating to indicate that chemotherapeutic agents may be selectively toxic to tumor cells because they increase oxidant stress and enhance these already stressed cells beyond their limit (8, 9). Cytotoxic ROS signaling seems to be mediated in part by activation of the apoptosis signal-regulating kinase 1 (ASK1)/mitogen-activated protein kinase (MAPK) signaling pathway (4, 10–12). ASK1, a member of the MAPK kinase kinase (MAPKKK) family, is an upstream activator of MAPK signaling cascades (12, 13). ASK1 is activated in response to various stresses, including tumor necrosis factor, serum withdrawal, endoplasmic reticulum stress, Fas ligation, and H₂O₂ (12, 14–17). ASK1 activity is regulated at multiple steps, including dimerization, phosphorylation, and protein-protein interactions (17, 18). The activation of ASK1 requires dimerization and consequent autophosphorylation, events that are modulated by several cellular stressors. Both 14-3-3 and thioredoxin bind to ASK1 and block its activity under nonstressed conditions (13, 19–21). H₂O₂ in turn triggers the dissociation of thioredoxin from ASK1 and is thus a potent stimulus for its activity (22, 23). Once activated, ASK1 can induce cell death by activating several proapoptotic signaling proteins, including c-jun-NH₂-kinase (JNK) and p38 MAPK (16, 24, 25).

Cinnamomum kotoense Kanehira & Sasaki (Lauraceae) is a small evergreen tree native to Lanyu Island of Taiwan that has recently been cultivated as an ornamental plant. Isoobtusilactone A (IOA; Fig. 1A) is a new butanolide constituent isolated from the leaves of *C. kotoense*, and its properties as an antitumor agent have not yet been fully described (26). This study is the first to determine the cell growth inhibition activity of IOA and examine its effect on cell cycle distribution and apoptosis in two human breast cancer cell lines, MCF-7 and MDA-MB-231. To further establish IOA's anticancer mechanism, we assayed the levels of cell cycle control- and apoptosis-related molecules, which are strongly associated with the programmed cell death signal transduction pathway and affect the chemosensitivity of tumor cells to anticancer agents.

Materials and Methods

Materials. FCS, RPMI 1640, penicillin G, streptomycin, and amphotericin B were obtained from Life Technologies BRL. DMSO, 2,3-bis[2-methoxy-4-nitro-5-sulphophenyl]-2*H*-tetrazolium-5-carboxanilide inner salt (XTT), RNase, trypsin-EDTA, and propidium iodide (PI) were purchased from Sigma Chemical. Dihydroethidium, 2',7'-dichlorodihydrofluorescein diacetate (H₂DCFDA), 5-chloromethylfluorescein diacetate (CMFDA), and JC-1 were obtained from Molecular Probes. ASK1, phospho-ASK1, extracellular signal-regulated kinase 1/2 (ERK1/2), phospho-ERK1/2, p38, phospho-p38, JNK, phospho-JNK, Bcl-2, Bcl-XL, Bax, and Bak antibodies were obtained from Cell Signaling Technology. Cyclin B1, cyclin A, cdc2, cdc25C, phospho-cdc2, phospho-cdc25C, and 14-3-3 antibodies were obtained from Santa Cruz

Requests for reprints: Ya-Ling Hsu, Department of Pharmacy, Chia-Nan University of Pharmacy and Science, Tainan, Taiwan. Phone: 886-6-266-4911, ext. 200; Fax: 886-6-2667318; E-mail: hsuyl326@gmail.com.

©2007 American Association for Cancer Research.
doi:10.1158/0008-5472.CAN-07-1089

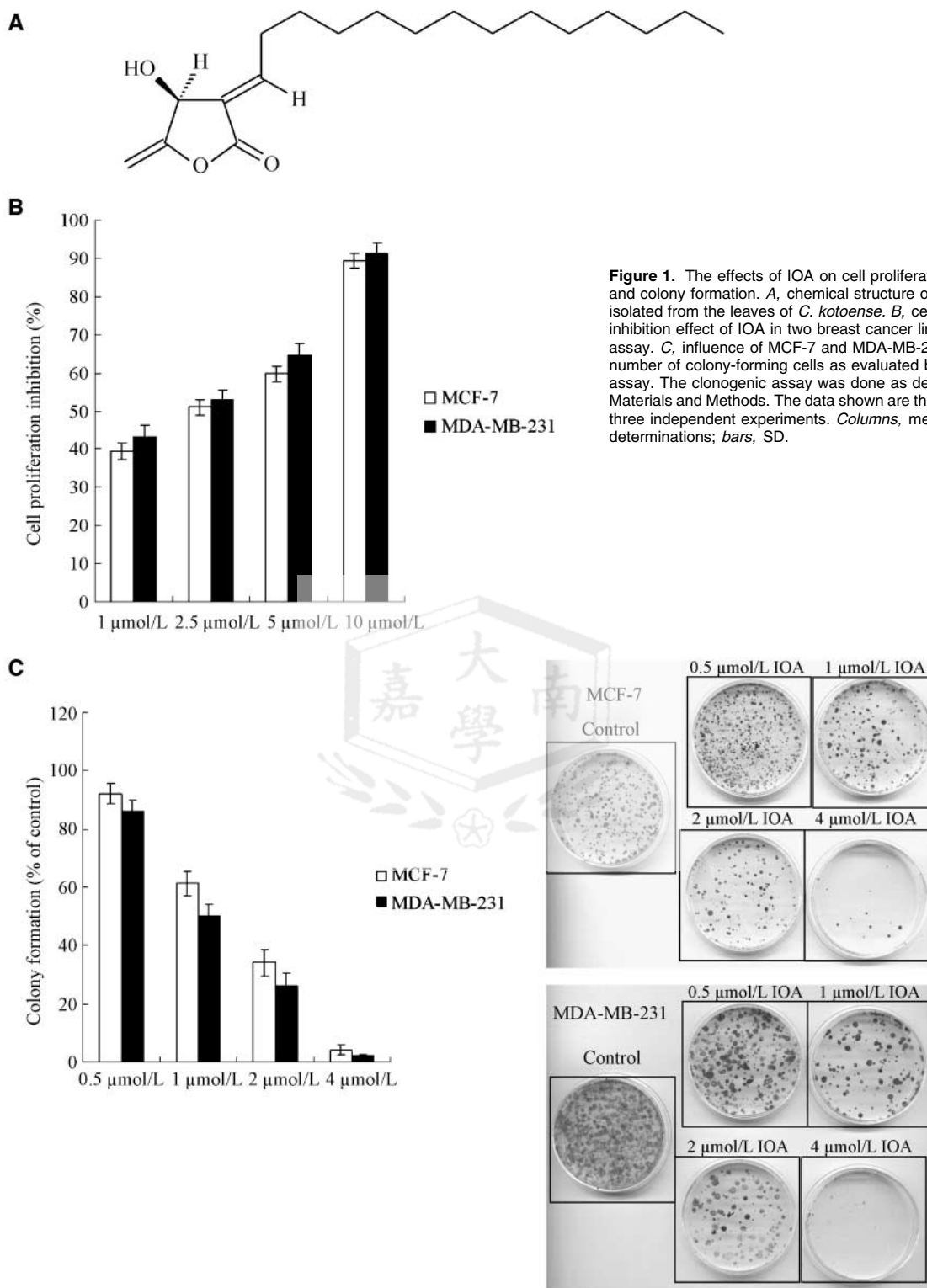


Figure 1. The effects of IOA on cell proliferation inhibition and colony formation. *A*, chemical structure of IOA isolated from the leaves of *C. kotoense*. *B*, cell proliferation inhibition effect of IOA in two breast cancer lines by XTT assay. *C*, influence of MCF-7 and MDA-MB-231 on the number of colony-forming cells as evaluated by clonogenic assay. The clonogenic assay was done as described in Materials and Methods. The data shown are the means from three independent experiments. *Columns*, mean of three determinations; *bars*, SD.

Biotechnology. ASK1 small interfering RNA (siRNA) plasmid was obtained from Upstate Biotechnology Inc. EUK8 and thioredoxin antibodies were purchased from Calbiochem.

Test compound. IOA was isolated from the leaves of *C. kotoense* as described previously (26). Briefly, the air-dried leaves were extracted

with methanol at room temperature, and the methanol extract was obtained upon concentration under reduced pressure. The methanol extract, suspended in H₂O, was partitioned with CHCl₃ to give fractions soluble in CHCl₃ and H₂O. The CHCl₃ soluble fraction was chromatographed over silica gel using *n*-hexane–EtOAc–acetone as eluent to produce

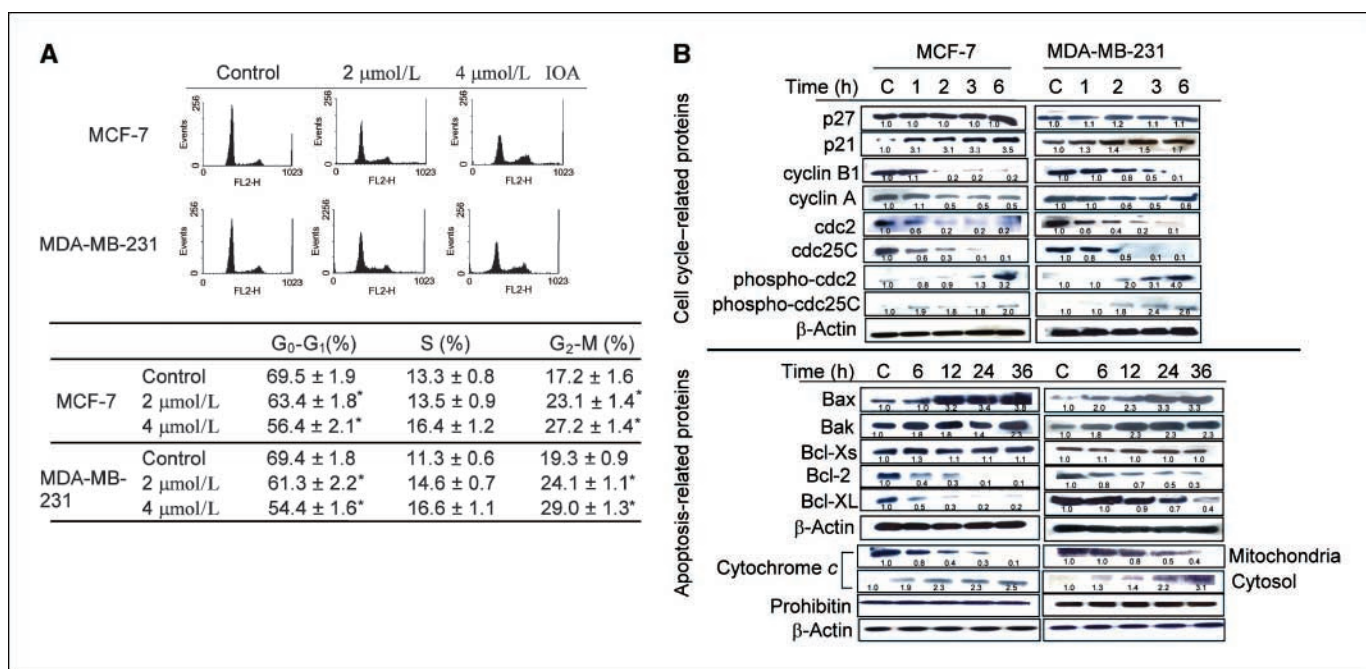


Figure 2. IOA-induced cell cycle arrest and apoptotic cell death in MCF-7 and MDA-MB-231. **A**, IOA caused cell cycle arrest at the G₂-M phase. Cells were treated with vehicle and IOA for 6 h, and cell cycle distribution was assessed by flow cytometry. **B**, The effect of IOA in cell cycle and apoptosis-related proteins. The various protein levels of 4 $\mu\text{mol/L}$ IOA-treated cancer cells were determined by immunoblot.

five fractions. Fraction I was further purified by another silica gel column using *n*-hexane-EtOAc to obtain IOA.

Cell culture. MCF-7 and MDA-MB-231 cells were obtained from the American Type Cell Culture Collection. MCF-7 cells were cultured in DMEM with nonessential amino acids, 0.1 mmol/L sodium pyruvate, 10 $\mu\text{g/mL}$ insulin, and 10% FCS. MDA-MB-231 cells were cultured in RPMI 1640 supplemented with 10% FCS and 1% penicillin-streptomycin solution.

Cell proliferation and clonogenic assay. Cells were plated in 96-well culture plates (1×10^4 cells per well). After 24 h incubation, the cells were treated with vehicle alone (0.1% DMSO) and various concentrations of IOA for 48 h. Inhibition of cell proliferation was measured by XTT assay as described previously (27). To determine long-term effects, cells were treated with IOA at various concentrations for 1 h. After being rinsed with fresh medium, cells were allowed to form colonies for 14 days, which were then stained with crystal violet (0.4 g/L; Sigma).

Cell cycle analysis. To determine cell cycle distribution analysis, 5×10^5 cells were plated in 60-mm dishes and treated with vehicle alone (0.1% DMSO) and various concentrations of IOA for 6 h. After treatment, the cells were stained with PI and analyzed by flow cytometer as described previously (27). The data were analyzed using Multicycle software (Phoenix Flow Systems).

Apoptosis assay. Cells (1×10^6) were treated with vehicle alone (0.1% DMSO) and various concentrations of IOA for 48 h. The cells were then collected and centrifuged at $500 \times g$ for 5 min. DNA was extracted from the cells as described previously (27). The DNA was separated in 2% agarose gel and visualized by UV after staining with ethidium bromide. Quantitative assessment of apoptotic cells was assessed by the terminal nucleotidyl transferase-mediated nick end labeling (TUNEL) method, which examines DNA strand breaks during apoptosis by using BD ApoAlert DNA Fragmentation Assay kit.

Measurements of ROS and glutathione. Levels of intracellular O₂ and H₂O₂ were assessed spectrofluorimetrically by oxidation of specific probes: dihydroethidium and H₂DCFDA. The amount of glutathione (GSH) was determined by CMFDA. Cells were exposed to 25 $\mu\text{mol/L}$ EUK8 alone, 5 mmol/L *N*-acetyl cysteine (NAC), 4 $\mu\text{mol/L}$ IOA alone, NAC plus IOA,

or EUK8 plus IOA for specified time intervals. The cells were stained with 10 $\mu\text{mol/L}$ H₂DCFDA, 10 $\mu\text{mol/L}$ dihydroethidium, and 25 $\mu\text{mol/L}$ CMFDA for 10 min at 37°C, and the fluorescence intensity of the cells was determined using the flow cytometer (26).

Assay for caspase-9 activity. The assay is based on the ability of the active enzyme to cleave the chromophore from the enzyme substrate of caspase-9, LEHD-pNA (Ac-Leu-Glu-His-Asp-pNA). Cell lysates were incubated with peptide substrate in assay buffer [100 mmol/L NaCl, 50 mmol/L HEPES, 10 mmol/L DTT, 1 mmol/L EDTA, 10% glycerol, 0.1% CHAPS (pH 7.4)] for 2 h at 37°C. The release of *p*-nitroaniline was monitored at 405 nm. Results are represented as the percentage of change in activity compared with the untreated control.

Mitochondrial membrane potential assay. We used mitochondrial-specific cationic dye JC-1, which undergoes potential-dependent accumulation in the mitochondria to check the change in mitochondrial membrane potential. Following treatment with various concentrations of IOA for the indicated times, cells were stained with 25 $\mu\text{mol/L}$ JC-1 for 30 min at 37°C. Fluorescence was monitored with the fluorescence plate reader at wavelengths of 490 nm (excitation)/540 nm (emission) and 540 nm (excitation)/590 nm (emission) pairs. Changes in the ratio between the measurement at test wavelengths of 590 nm (red) and 540 nm (green) fluorescence intensities are indicative of changes in the mitochondrial membrane potential (27).

Immunoprecipitation/immunoblot and JNK and p38 activity assays. Immunoblot analysis was carried out as described previously (27). Mitochondrial and cytoplasmic fractions were separated using Cytochrome *c* Releasing Apoptosis Assay kit (BioVision). After equivalent amounts of protein were resolved by SDS-PAGE (10–12%) and transferred to polyvinylidene difluoride membranes, membranes were blocked with 5% nonfat dry milk in TBS and incubated with the desired primary antibody for 1 to 16 h. The membrane was then treated with appropriate peroxidase-conjugated secondary antibody, and the immunoreactive proteins were detected using an enhanced chemiluminescence kit (Amersham). Quantification was made using a digital image analysis system (SigmaGel software).

For association of ASK1 with thioredoxin or 14-3-3, cell lysates (300 μg) were incubated with 10 μL anti-thioredoxin or anti-14-3-3 antibodies for 1 h

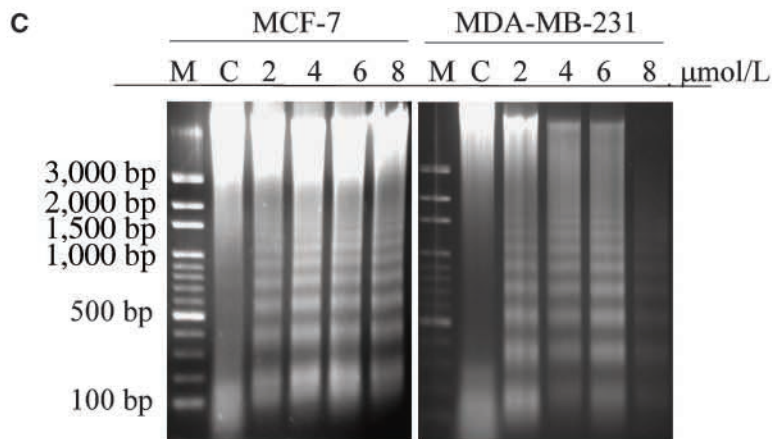
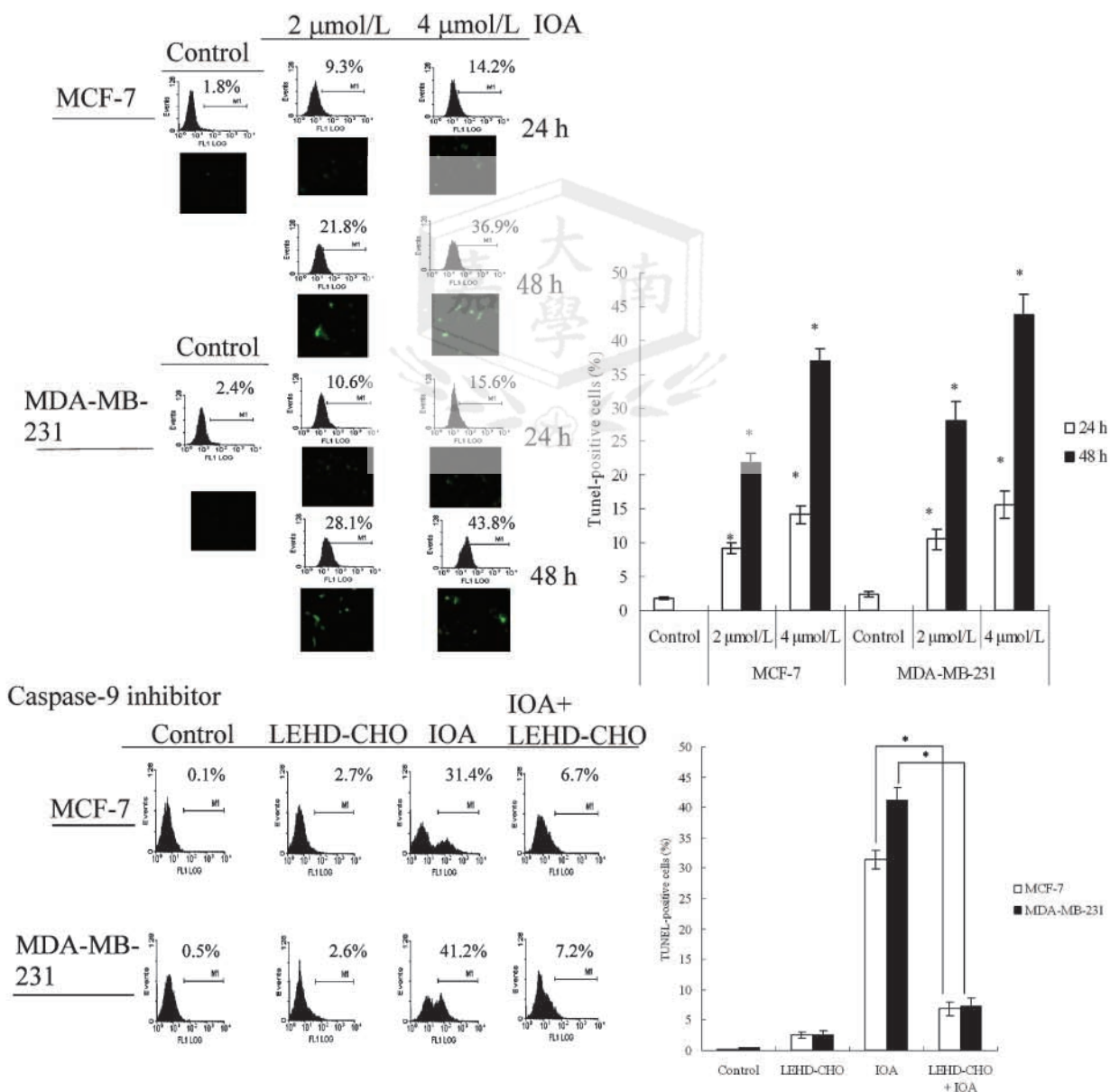


Figure 2 Continued. C, IOA-induced MCF-7 and MDA-MB-231 cells undergo apoptosis, which was inhibited by caspase-9 inhibitor. The induction of apoptosis was determined at 48 h by agarose gel electrophoresis and TUNEL assay at 24 and 48 h. For blocking assay, cells were preincubated with or without LEHD-CHO (20 μmol/L) for 1 h before the addition of 4 μmol/L IOA for an additional 48 h.



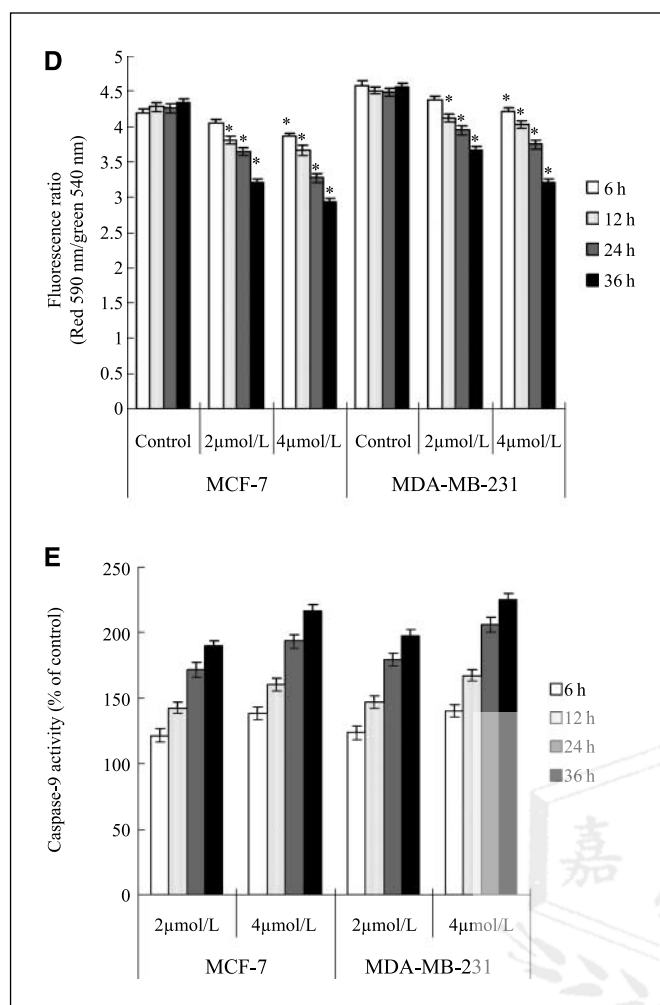


Figure 2 Continued. D, the loss of $\Delta\Psi_m$, which was measured by JC-1. E, the activation of caspase-9. Results shown are representative of three independent experiments. *, $P < 0.05$, significant difference between two test groups as analyzed by Dunnett's test.

at 4°C. Immunocomplexes were resolved by 7.5% SDS-PAGE. Association of thioredoxin or 14-3-3 with ASK1 was detected by incubating the blots with anti-ASK1 antibodies. The JNK and p38 activities were determined using kits from Cell Signaling Technology according to the manufacturer's instructions.

siRNA-based knockdown of ASK1, JNK, and p38 expression. Breast cancer cell monolayers were transfected with ASK1 siRNA expression plasmid pKD-Ask1-v2, pKD-NegCon-v1, SMARTpool p38/SPAK, JNK1 siRNA duplexes or nonspecific control siRNA duplexes (Upstate Biotechnology Inc.) using LipofectAMINE 2000 (Invitrogen). Immunoblot analyses showed that ASK1, JNK, and p38 all remained low but detectable, and expression of β -actin was unaffected by plasmid or siRNA transfection.

In vivo tumor xenograft study. Female nude mice [6 weeks old; BALB/cA-nu (*nu/nu*)] were purchased from the National Science Council Animal Center (Taipei, Taiwan) and maintained in pathogen-free conditions. MDA-MB-231 cells were injected s.c. into the flanks of these nude mice (5×10^6 cells in 200 μ L), and tumors were allowed to develop for ~30 days until they reached ~200 mm³, when treatment was initiated. Twenty mice were randomly divided into two groups. The mice in the IOA-treated group were i.p. injected daily with IOA in a clear solution containing 25% polyethylene glycol (PEG; 4 mg/kg of body weight) in a volume of 0.2 mL. The control group was treated with an

equal volume of vehicle. After transplantation, tumor volume was measured using calipers and estimated according to the formula: tumor volume (mm³) = $L \times W^2/2$, where L is the length, and W is the width. Tumor-bearing mice were sacrificed after 45 days. Xenograft tumors, as well as other vital organs of the treated and control mice, were harvested and fixed in 4% formalin, embedded in paraffin, and cut into 4- μ m sections for histologic study.

Statistical analysis. Data were expressed as means \pm SD. Statistical comparisons of the results were made using ANOVA. Significant differences ($P < 0.05$) between the means of control and IOA-treated cells or two test groups were analyzed by Dunnett's test.

Results

IOA inhibits cell proliferation and clonogenic survival in MCF-7 and MDA-MB-231 cells. To investigate the potential cell growth inhibition of IOA in breast cancer, we first examined the effect of IOA on cell proliferation and clonogenic survival in MCF-7 and MDA-MB-231 cells. As shown in Fig. 1B, IOA inhibited cell growth in both cancer cell lines in a concentration-dependent manner. The IC₅₀ values of IOA were 2.1 μ mol/L for MCF-7 and 1.8 μ mol/L for MDA-MB-231.

Additional experiments were done to determine the antitumor activities of IOA by clonogenic assays. *In vitro* clonogenic assays correlated very well with *in vivo* assays of tumorigenicity in nude mice (28). Figure 1C shows the effects of IOA on the relative clonogenicity of the control and the IOA-treated MCF-7 and MDA-MB-231 cells. Clonogenicity of both cancer cell lines was reduced in a concentration-dependent manner after exposure to IOA.

IOA induces cell cycle arrest and regulates the expression of cell cycle-related proteins. To examine the mechanism responsible for IOA-mediated cell growth inhibition, cell cycle distribution and related regulatory factors were assessed. The results showed that treating cells with IOA caused a significant inhibition of cell cycle progression in both cancer cell lines at 6 h (Fig. 2A), resulting in a clear increase in the percentage of cells in the G₂-M phase when compared with the control. Figure 2B shows that IOA treatment of the cells resulted in a time-dependent decrease in the protein expression of cyclin A, cyclin B1, cdc2, and cdc25C in both cancer cell lines (Fig. 2B). In addition, exposure of cells to IOA resulted in an increase in levels of inactive phospho-cdc2 (Tyr¹⁵) at 3 h and phospho-cdc25C (Ser²¹⁶) at 1 to 2 h. Results from time-dependent studies have indicated that decreasing functional cdc25C by increasing phosphorylation of cdc25C was followed by an increase in phospho-cdc2 (Fig. 2B). We suggest that cdc2 action was inhibited by a decrease in cdc25C expression. Moreover, IOA treatment also increased the expression of CDK inhibitor p21 in both cell lines.

IOA induces apoptosis through the activation of the mitochondrial pathway. We next assessed the effect of IOA on the induction of apoptosis in MCF-7 and MDA-MB-231 by DNA fragmentation assay. The results showed that IOA treatment results in the formation of DNA fragments at 48 h in both cell lines, as determined by agarose gel electrophoresis (Fig. 2C). A quantitative evaluation was also made using TUNEL to detect DNA strand breaks. Compared with vehicle-treated cells, 4 μ mol/L IOA at 48 h induced 36.9% and 43.8% apoptosis in MCF-7 and MDA-MB-231 cells, respectively (Fig. 2C). TUNEL-positive cells were also visible using a fluorescence microscope (Fig. 2C).

To investigate the mitochondrial apoptotic events involved in IOA-induced apoptosis, we analyzed the changes in the Bcl-2

family proteins, cytochrome *c* store, mitochondrial membrane potential ($\Delta\Psi_m$) and caspase-9 activity. Immunoblot analysis showed that treatment of MCF-7 and MDA-MB-231 cells with IOA increased Bax and Bak protein levels (Fig. 2B). In contrast, IOA decreased Bcl-2 and Bcl-XL levels, which led to an increase in the proapoptotic/antiapoptotic Bcl-2 ratio (Fig. 2B). IOA failed to affect the expression of Bcl-Xs. The cytosolic fraction from untreated breast cancer cells contained no detectable amounts of cytochrome *c*, whereas it did become detectable after 4 $\mu\text{mol/L}$ IOA treatment in both MCF-7 and MDA-MB-231 cells (Fig. 2B). In addition, we investigated mitochondrial dysfunction by measuring $\Delta\Psi_m$ in IOA-treated breast cancer cells for the indicated times (Fig. 2D).

Hallmarks of the apoptotic process include the activation of cysteine proteases, which represent both initiators and executors of cell death (29). Upstream caspase-9 activities increased significantly, as shown by the observation that treatment with IOA increased caspase-9 activity in both MCF-7 and MDA-MB-231 cells (Fig. 2E). This is consistent with the release of cytochrome *c* into the cytosol. Furthermore, when cells were pretreated with the specific caspase-9 inhibitor LEHD-CHO before IOA treatment, the apoptosis induction effect of IOA decreased in both MCF-7 and MDA-MB-231 cells (Fig. 2C).

The effect of IOA on the generation of ROS and GSH and thioredoxin levels. Dysregulation of cellular redox status can be a potent mechanism of cell death (7). Therefore, we tested the possibility that IOA induces apoptosis allowing for ROS accumulation. Fluorescence-activated cell sorting (FACS) detection revealed that intracellular O_2^- and H_2O_2 levels increased in both MCF-7 and MDA-MB-231 cells following treatment with 2 and 4 $\mu\text{mol/L}$ IOA for 2 h (Fig. 3A). EUK8, a synthetic salen-manganese complex with high superoxide dismutase (SOD) and catalase-mimic activities, completely blocked the generation of H_2O_2 induced by IOA. In addition, IOA-induced H_2O_2 was also decreased by NAC, a ROS scavenger in cells, by interacting with $\text{OH}\cdot$ and H_2O_2 (Fig. 3A).

Because GSH scavenges ROS in cells by interacting with $\text{OH}\cdot$ and H_2O_2 (30), thereby affecting ROS-mediated signaling pathways, we next examined the levels of GSH in IOA-treated cells. Results showed that intracellular GSH levels decreased in both MCF-7 and MDA-MB-231 cell lines following treatment with 4 $\mu\text{mol/L}$ IOA for 2 h treatment (Fig. 3A). Thioredoxin functions as a hydrogen donor for many protein targets and is the major scavenger for ROS (30), so we also assessed the changes of thioredoxin levels in IOA-treated cells. As shown in Fig. 3B, IOA decreased the expression of thioredoxin in both MCF-7 and MDA-MB-231 cells. Decreased levels of thioredoxin are associated with reduced GSH and increased ROS accumulation.

The effect of IOA in ASK1/MAPK signaling. Because it has been shown that ROS-mediated DNA damage triggers activation of MAPK and subsequent cell death (30), we assessed the status of MAPK signaling after IOA treatment. First, ASK1 activation (phosphorylation at the activation loop Thr⁸⁴⁵ and dephosphorylation at Ser⁹⁶⁷) was assessed by immunoblot analysis. Treatment of either MCF-7 or MDA-MB-231 cells with IOA significantly increased ASK1 phosphorylation (Thr⁸⁴⁵) concomitant with reduction of inactive ASK1 phosphorylation (Ser⁹⁶⁷). The change of active/inactive ASK1 was evident as early as 1 h after IOA treatment (Fig. 3B). In addition, results also showed that exposure of either line of breast cancer cells to 4 $\mu\text{mol/L}$ IOA resulted in a rapid and sustained activation of p38 and JNK. Activation

(phosphorylation) of p38 and JNK was determined after 1 h treatment and persisted for the duration of the experiment. On the other hand, the expression of p38 and JNK (unphosphorylated form) was not altered by IOA treatment. However, IOA only slightly affected ERK1/2 activation in either MCF-7 or MDA-MB-231 cells at any of the examined points in time (Fig. 3B). IOA-mediated activation of p38 and JNK was additionally confirmed by determining phosphorylation of one of its substrates [activating transcription factor (ATF)-2 and c-Jun for p38 and JNK, respectively]. As shown in Fig. 3C, in contrast with the control, the Ser⁶³ phosphorylation of c-Jun increased after a 1-h exposure of MCF-7 and MDA-MB-231 cells to 4 $\mu\text{mol/L}$ IOA. Similarly, phosphorylation of ATF-2 at Thr⁷¹ increased in both IOA-treated MCF-7 and MDA-MB-231 cells, in contrast to the control (Fig. 3C).

We next assessed the association of endogenous thioredoxin and 14-3-3 with ASK1 by immunoprecipitation with anti-thioredoxin or anti-14-3-3 antibodies followed by immunoblot with anti-ASK1 antibodies. Figure 3D shows that the association of thioredoxin and ASK1 decreased in a time-dependent manner in IOA-treated MCF-7 and MDA-MB-231 cells. Similarly, the association of 14-3-3 protein was also reduced by IOA treatment (Fig. 3D).

The role of ROS in IOA-mediated ASK1 activation and apoptosis. To understand the mechanism by which ROS enhance ASK1 activation, we next determined the role of ROS in the dissociation of ASK1 from its inhibitors thioredoxin and 14-3-3 and the activation of ASK1. Cells were treated with the EUK8, NAC, EUK8 plus IOA, or NAC plus IOA. Association of ASK1 with thioredoxin or 14-3-3 was then determined by immunoprecipitation. The results showed that pretreatment with EUK8 and NAC caused a significant inhibition of IOA-induced dissociation of ASK1 with thioredoxin and 14-3-3 protein, as well as the phosphorylation of ASK1 at Thr⁸⁴⁵ and dephosphorylation at Ser⁹⁶⁷ in both cell lines (Fig. 4A).

Next, we further assessed the effect of antioxidant agents in IOA-induced apoptosis. The results showed that IOA-induced apoptosis, in both cell lines, was significantly attenuated in EUK8 or NAC-pretreated cells, compared with IOA-treated MCF-7 and MDA-MB-231 cells. These data strongly suggest that the generation of ROS plays an important role in IOA-induced apoptosis (Fig. 4B).

The role of ASK1 pathway in IOA-mediated MAPK activation and apoptosis. To confirm the central role of the ASK1 as a key upstream of IOA-mediated JNK and p38 activation, we transfected MCF-7 and MDA-MB-231 with pKD-ASK1-v2 plasmid that constitutively expresses short hairpin RNAs targeting ASK1. As shown in Fig. 4C, ASK1 siRNA reduced ASK1 expression ~70% in comparison with control siRNA. Selective genetic inhibition of ASK1 abrogated the phosphorylation of JNK (Fig. 4C). Similar to JNK activation, IOA-induced p38 activation was specifically blocked by ASK1 inhibition, suggesting that ASK1 is a potential upstream activator of JNK and p38 signaling (Fig. 4C).

To determine whether ASK1 is also involved in IOA-induced cell death, ASK1 knockdown-MCF-7 and MDA-MB-231 were treated with IOA (4 $\mu\text{mol/L}$), and then apoptotic rate was determined by TUNEL. The results showed that specific knockdown ASK1 expression by ASK1 siRNA also inhibited IOA-mediated apoptosis. These data clearly indicate that the activation of ASK1 might act as upstream of JNK and p38 and plays a key role in IOA-induced apoptosis (Fig. 4D).

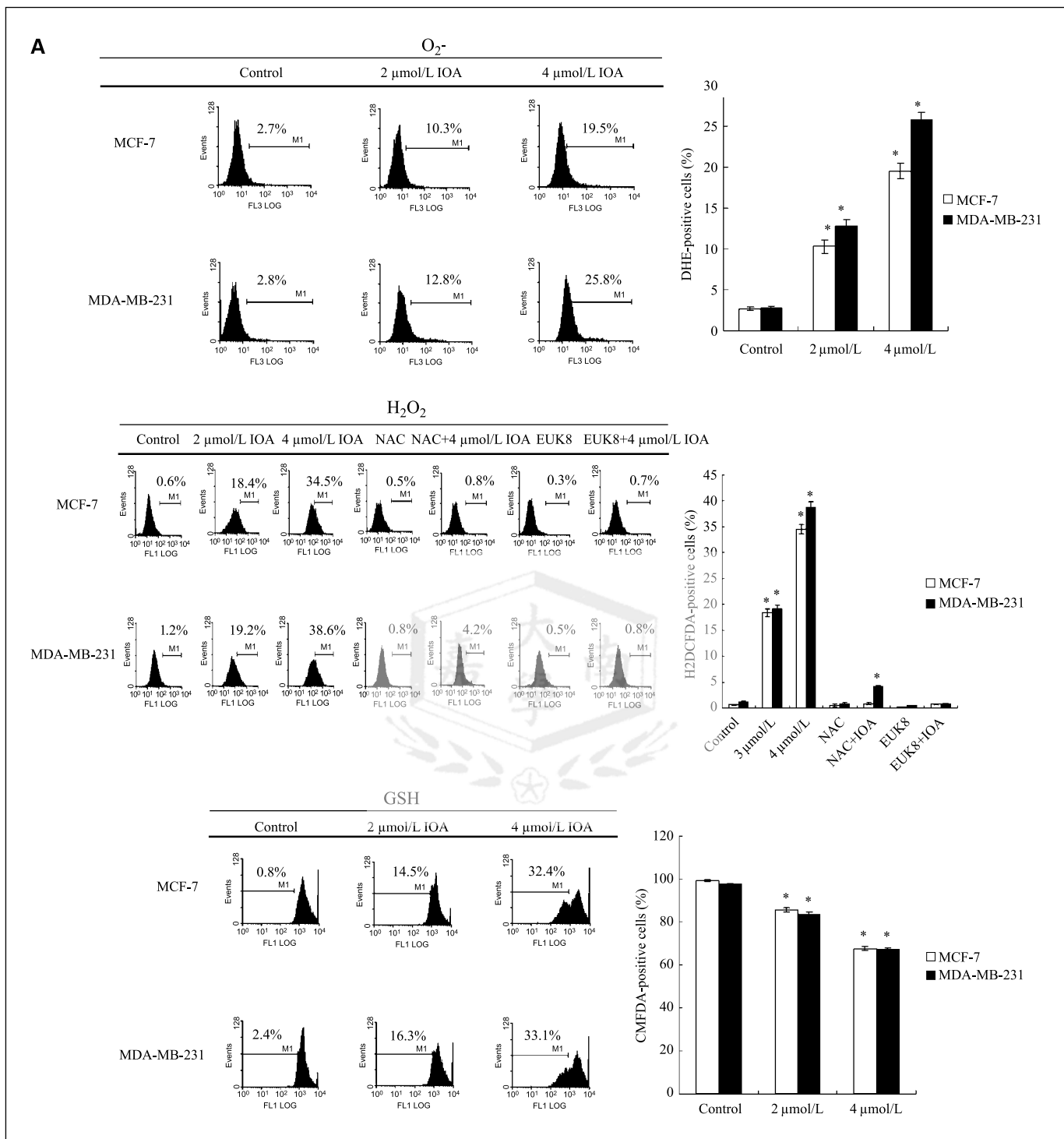


Figure 3. The effect of IOA on the production of ROS, the decrease of GSH and thioredoxin, and the activation of ASK1/MAPK pathway. **A**, the effect of IOA on the production of O₂⁻, the generation of H₂O₂, and the levels of cellular GSH. Cells were exposed to 25 μmol/L EUK8 alone, 5 mmol/L NAC, 4 μmol/L IOA alone, NAC plus IOA, or EUK8 plus IOA for 2 h. The amounts of H₂O₂, O₂⁻ and GSH were assayed by H₂DCFDA (for H₂O₂), dihydroethidium (for O₂⁻), and CMFDA (for GSH) staining.

Genetic inhibition of p38 and JNK blocks IOA-mediated cell cycle arrest and apoptosis. We further investigated the mechanism that accounts for the actions of JNK and p38 in IOA-induced apoptosis in breast cancer cells. Therefore, we employed genetic inhibition to specifically inhibit p38 and JNK to assess the consequences of p38 and JNK inhibition on IOA-mediated cell cycle arrest

and apoptosis. To do so, MCF-7 and MDA-MB-231 cells were transfected with a pool of siRNAs targeting p38 or JNK1, after which the cells were exposed to 4 μmol/L IOA for a specific time. As shown in Fig. 5A, in comparison with oligonucleotide-transfected control cells, transfection of cells with p38 and JNK1 siRNA reduced basal amounts of p38 and JNK1. Selective genetic

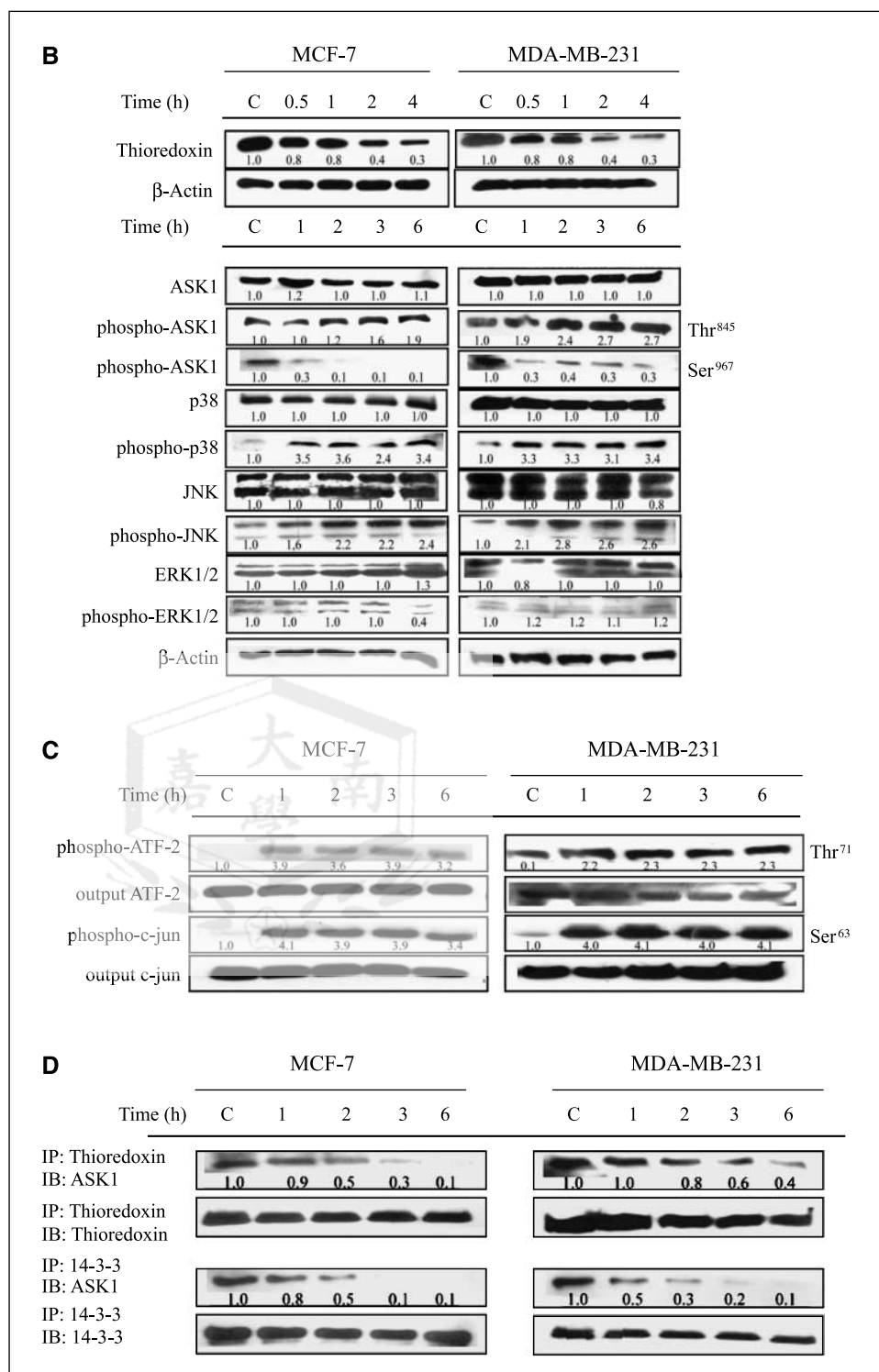


Figure 3 Continued. B, IOA decreased the amount of thioredoxin and increased the activation of ASK1/MAPK. Cells were treated with 4 μmol/L IOA for the indicated times, and the levels of various proteins were assessed by immunoblot assay. C, IOA enhanced the activity of JNK and p38, as determined by JNK and p38 activity kit. D, IOA decreased the association of ASK1 with thioredoxin or 14-3-3 proteins. The association of ASK1 with thioredoxin or 14-3-3 proteins was determined by immunoprecipitation assay. Results shown are representative of three independent experiments. *, $P < 0.05$, significant difference between control and IOA-treated group as analyzed by Dunnett's test.

inhibition of p38 not only blocked IOA-induced G₂-M phase arrest, but also abrogated phosphorylation of cdc25C as well as the degradation of this protein (Fig. 5B and D). In contrast, JNK inhibition failed to affect either the IOA-mediated G₂-M arrest and changes in cdc25C expression or its phosphorylation in either MCF-7 or MDA-MB-231 (Fig. 5B and D). On the other hand, specific knockdown JNK1 expression by JNK1 siRNA inhibited IOA-

mediated apoptosis (Fig. 5C). In addition, IOA-mediated up-regulation of Bax and down-regulation of Bcl-2 were significantly prevented by specific siRNA inhibition of JNK in both MCF-7 and MDA-MB-231 cell lines (Fig. 5D). However, p38 inhibition slightly inhibited the induction of apoptosis and the change of Bax/Bcl-2 in either MCF-7 or MDA-MB-231 cells (Fig. 5C and D). The consequences of p38 and JNK1 inhibition by genetic inhibition on

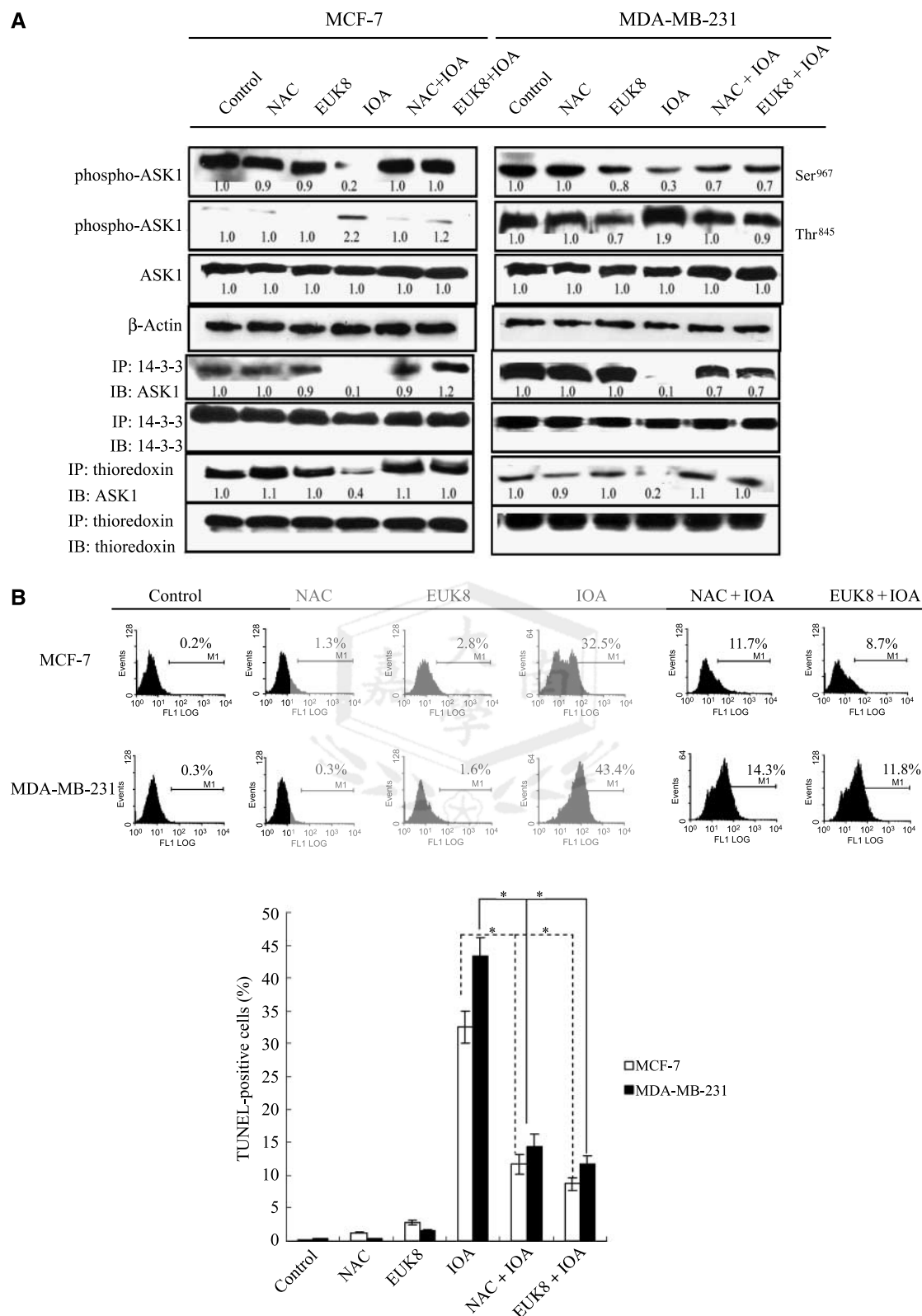


Figure 4. The role of ROS and ASK1 on the IOA-induced apoptosis. **A**, antioxidants inhibited IOA-mediated ASK1 phosphorylation at Thr⁸⁴⁵ and dephosphorylation at Ser⁹⁶⁷ and the association of ASK1 with thioredoxin and 14-3-3 proteins. **B**, antioxidants inhibited IOA-mediated apoptosis. Cells were incubated for 1 h in the presence or absence of EUK8 and NAC, and then 4 μ mol/L IOA was added and incubated for specific times (3 h for ASK1 phosphorylation and association activity and 48 h for apoptosis assay). The induction of apoptosis was estimated by TUNEL analysis. Phosphorylated ASK1 levels were assessed by immunoblot assay. The association of ASK1 with thioredoxin or 14-3-3 proteins was determined by immunoprecipitation assay.

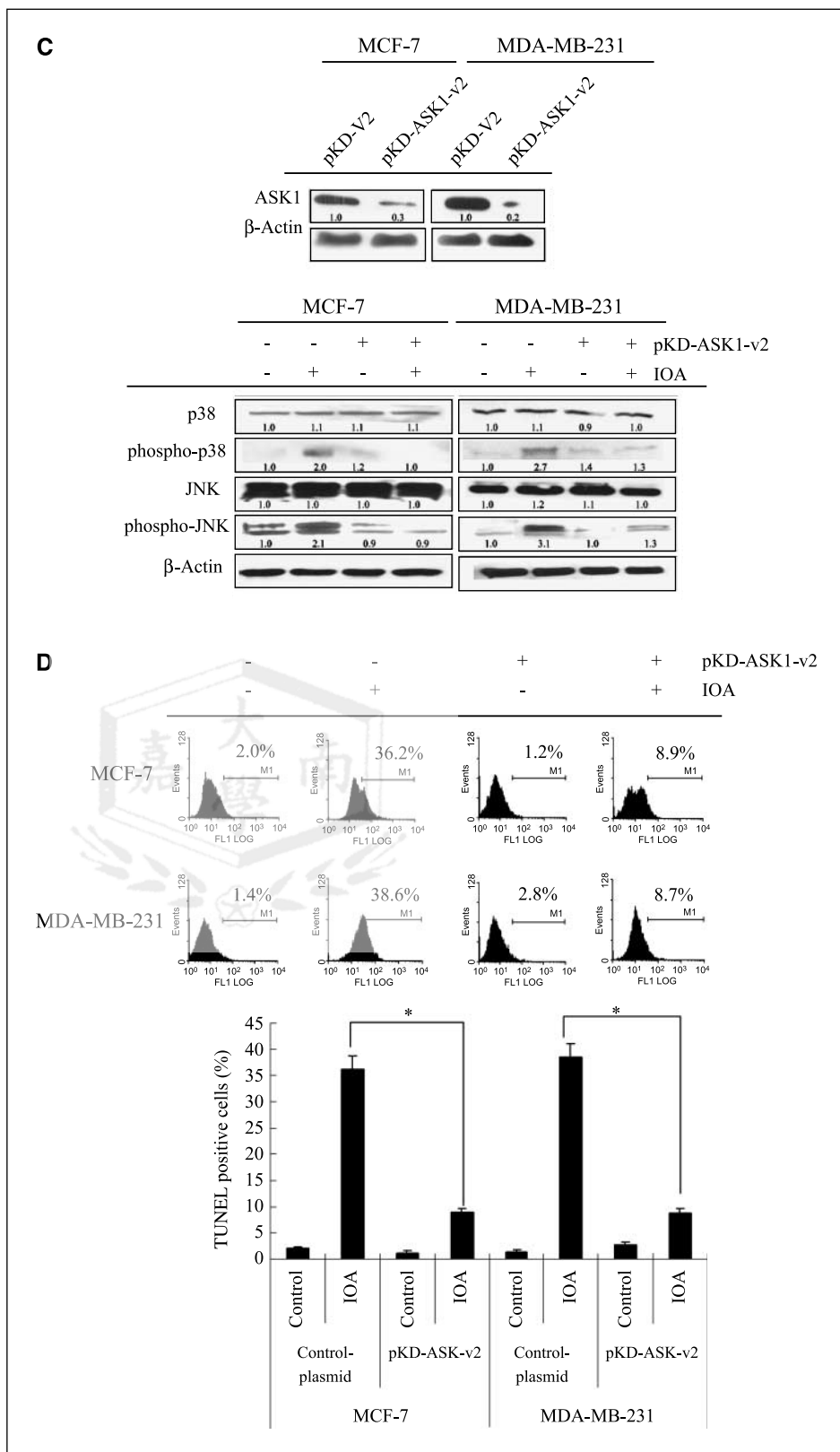


Figure 4 Continued. C, genetic suppression of ASK1 by pKD-ASK1-v2 plasmid transfection, and inhibition of ASK1 decreased the activation of JNK and p38. D, inhibition of ASK1 decreased IOA-induced apoptosis. For (C) and (D), cells were transfected with control plasmid or pKD-ASK1 plasmid by LipofectAMINE 2000 agents and then treated with IOA for the indicated times (3 h for p38 and JNK expression and 48 h for apoptosis assay). Protein expression and apoptosis were assessed as described above. Each value is the mean \pm SD of three determinations. *, $P < 0.05$, significant difference between two test groups as analyzed by Dunnett's test.

IOA-mediated G₂-M arrest and apoptosis induction showed that p38 and JNK may play important roles in molecular regulation.

IOA inhibits tumor growth in nude mice. To determine whether IOA inhibits tumor growth *in vivo*, equal numbers of

MDA-MB-231 cells were injected s.c. into both flanks of the nude mice. Tumor growth inhibition was most evident in mice treated with IOA at 4 mg/kg/day, where an ~50% reduction in tumor size was observed, in contrast with mice treated with vehicle

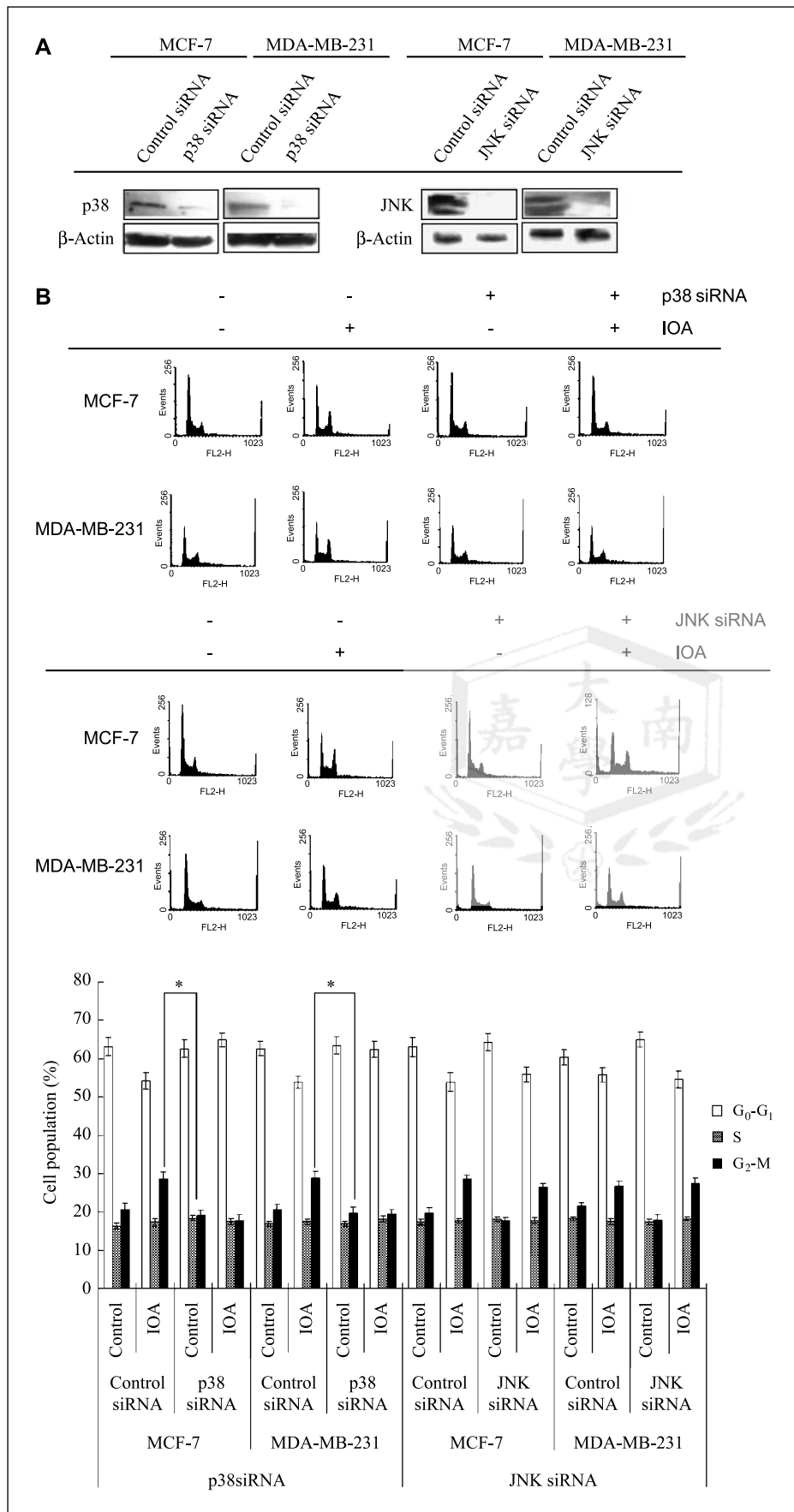


Figure 5. A, genetic suppression of p38 and JNK1 by p38 siRNA and JNK siRNA transfection. B, the effect of p38 and JNK siRNA inhibition on IOA-mediated G₂-M arrest.

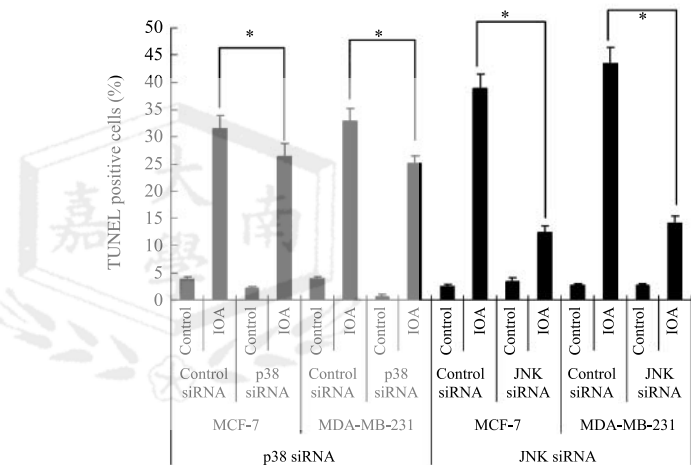
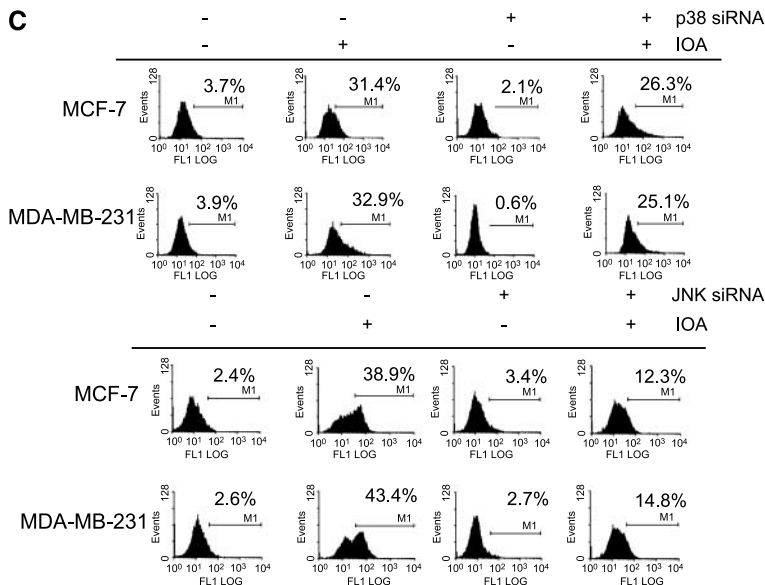
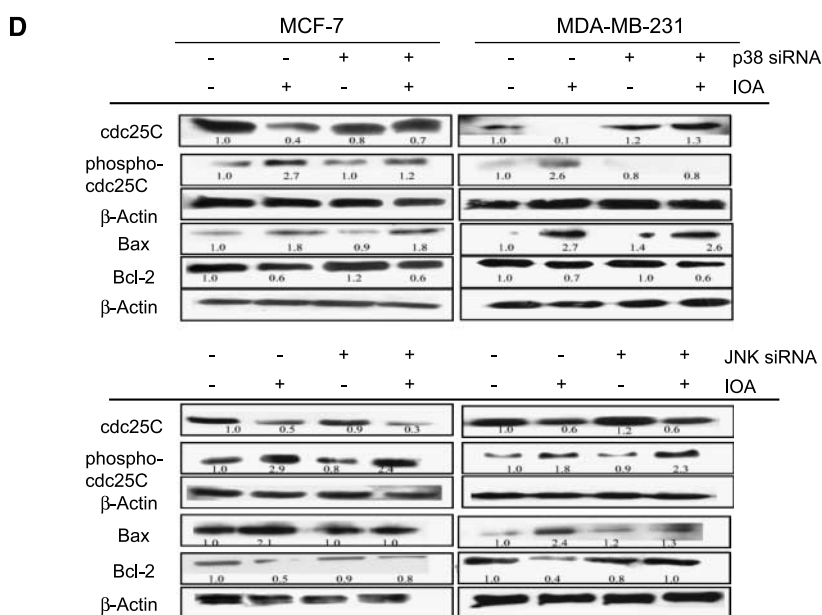


Figure 5 Continued. C, the effect of p38 and JNK siRNA inhibition on IOA-mediated apoptosis. D, the effect of p38 and JNK siRNA inhibition on the expressions of cdc25C and Bcl-2 family proteins after IOA treatment. Cells were transfected with control oligonucleotide, p38, or JNK1 siRNA by LipofectAMINE 2000 agents and then treated with IOA for the indicated times (3 h for p38, JNK expression, and cell cycle-related proteins 6 h for cell cycle analysis, 12 h for Bcl-2 family protein, and 48 h for apoptosis assay). The various protein expressions, cell cycle distribution, and apoptosis induction were assessed as described above. Each value is the mean \pm SD of three determinations. *, $P < 0.05$, significant difference between two test groups as analyzed by Dunnett's test.



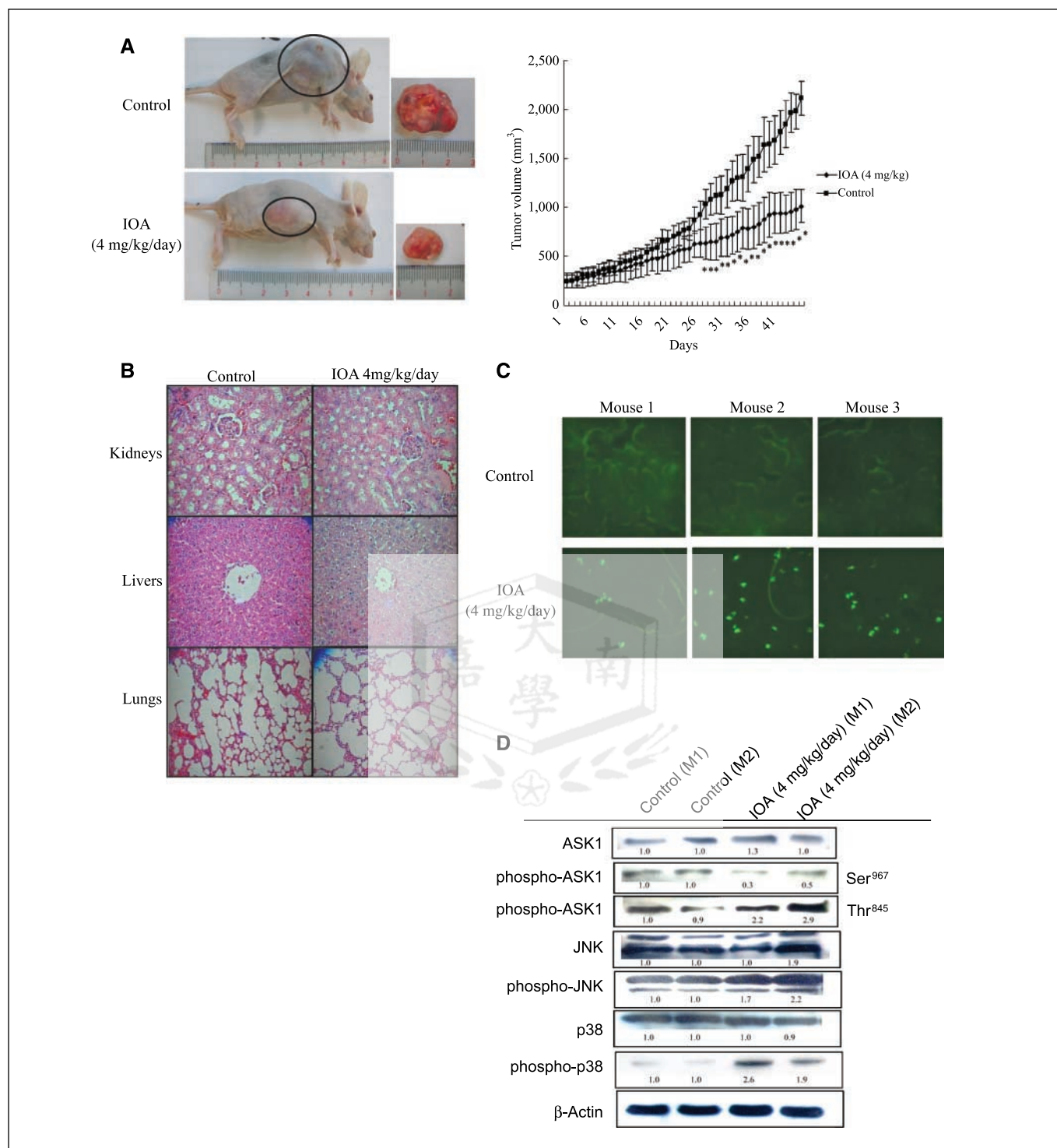


Figure 6. IOA inhibits growth and induces apoptosis of MDA-MB-231 xenograft by increasing ASK1 activation. **A**, mean of tumor volume measured at the indicated number of days after implant. **B**, tissue sections of livers, lungs, and kidneys of IOA-treated nude mice determined by H&E stain. **C**, IOA induces apoptosis in MDA-MB-231 xenograft as determined by TUNEL assay. **D**, the effect of IOA on the phosphorylation of ASK1, p38, and JNK. MDA-MB-231 xenograft. Animals bearing pre-established tumors ($n = 10$ per group) were dosed daily for 45 d with i.p. injections of IOA (4 mg/kg/day) or vehicle. During the 45-d treatment, tumor volumes were estimated using measurements taken by external calipers (mm³). Apoptosis was assessed by TUNEL assay. The levels of various proteins were assessed by immunoblot analysis. *, $P < 0.05$, significant difference between two test groups as analyzed by Dunnett's test.

(Fig. 6A). No sign of toxicity, as judged by parallel monitoring of body weight and tissue sections of lungs, livers, and kidneys, was observed in IOA-treated mice (Fig. 6B). In addition, an increase of TUNEL-positive cells was observed in tumors of the IOA-treated

mice when compared with tumors taken from vehicle-treated mice (Fig. 6C). An increase of phospho-ASK1, phospho-JNK, and phospho-p38 was also observed in tumors from the IOA-treated group (Fig. 6D).

Discussion

Breast cancer is the most common neoplasm in women of both developed and developing countries (1). This study is the first to find that IOA effectively inhibits tumor cell growth of two breast cancer cell lines, MCF-7 and MDA-MB-231, *in vitro*, concomitant with induction of cell cycle arrest and apoptosis, and inhibits tumor cell growth in nude mice.

Mitochondrial apoptotic pathway has been described as an important signaling of apoptotic cell death for mammalian cells (29). Following the treatment of MCF-7 and MDA-MB-231 cells with IOA, we observed that IOA treatment resulted in a significant increase of Bax and Bak expression and a decrease of Bcl-2 and Bcl-XL, suggesting that changes in the ratio of proapoptotic and antiapoptotic Bcl-2 family proteins might contribute to the apoptosis-promotion activity of IOA. Our findings also showed a collapse of $\Delta\Psi_m$, a substantial release of cytochrome *c*, and the activation of caspase-9 after breast cancer cells were treated with IOA. These mitochondrial apoptotic events are correlated with the modulation of IOA on Bcl-2 family proteins. The importance of this pathway was further confirmed by the protection from programmed cell death that is conferred by caspase-9 inhibition.

A large number of studies have established that the enhancement of oxidative stress is associated with the apoptotic response induced by several anticancer agents (7, 30–33). The status of intracellular redox is regulated by antioxidant enzymes (SOD, catalase, and glutathione peroxidase) and nonenzymatic thiol-disulfide redox buffers (GSH, vitamin C, thioredoxin; refs. 30, 34). They have been found to play a protective role through detoxification and modulation of the cellular redox state, and the subsequent trigger redox-sensitive signaling pathways and interaction with pro- and antiapoptotic signals (34). High levels of GSH and thioredoxin have been reported in a wide range of human cancers and are associated with cancers resistant to therapy (35, 36). Because the level of GSH and thioredoxin is an important factor in protection against apoptosis, the efficacy of anticancer drug-induced apoptosis requires depletions of GSH and thioredoxin, thus facilitating cancer cell death (26, 35, 36). In this study, we have shown that treatment of either MCF-7 or MDA-MB-231 cell lines with IOA resulted in reductions of GSH and thioredoxin followed by accumulation of O_2^- and H_2O_2 . Furthermore, we observed that the blocking enhancement of ROS by NAC and EUK8 decreased IOA-induced apoptosis, suggesting that ROS accumulation contributes to IOA-induced cell death in human breast cancer cells.

A number of studies have reported that MAPK signaling cascades play an important role in oxidative stress-induced apoptotic cell death (13, 30). ASK1 is an upstream activator of JNK and p38, which have been shown to be involved in the regulation of cell cycle and induction of apoptosis (13, 25, 30). Several cellular factors, including thioredoxin and 14-3-3, have been reported to interact with different ASK1 domains and to inhibit ASK1 activity (19, 22). The release of thioredoxin and 14-3-3 from ASK1 seems to be a critical step in ASK1 activation (19, 22). The oligomerization of free ASK1 leads to autophosphorylation of ASK1 at Thr⁸⁴⁵ within the activation loop in the kinase domain and subsequently recruits and activates its downstream targets MAPKK (MKK3/6 and MKK4/7) and MAPK (JNK and p38; refs. 15, 19, 22). Our study found that IOA-induced ROS was involved in the decrease of inactive phosphorylation ASK1 at Ser⁹⁶⁷ and release of ASK1 from inhibitor 14-3-3 and thioredoxin, resulting in ASK1

activation. These effects, however, were canceled in MCF-7 and MDA-MB-231 cells that were cotreated with IOA and antioxidant agents (EUK8 and NAC). Moreover, selective knockdown ASK1 expression by siRNA-based inhibition approach also decreased the effects of IOA on the activation of JNK, p38, and apoptosis, suggesting that the cooperation of ROS with ASK1 plays a crucial role in IOA-induced cell death in human breast cancer cells.

Recent studies have shown that MAPK signaling pathways regulate the eukaryotic cell cycle. p38 has been shown as essential for sustained G₂-M arrest induced by various anticancer agents (37–40). Reduced activity of cdc25C and a subsequent increase in cdc2 phosphorylation led to cell cycle arrest at the G₂-M phase (41). In this study, we found that the activation of p38 was involved in the accumulation of inactive phospho-cdc2, which may be due to the decrease of cdc25C activation by phosphorylation, leading to subsequent G₂ arrest. These effects, however, were abolished in MCF-7 and MDA-MB-231 cell lines that selectively knocked down p38 expression by p38 siRNA-based inhibition. These data suggest that p38 plays a key role in IOA-mediated G₂-M arrest. Activation of the JNK pathways has long been associated with the apoptotic response induced by several DNA-damaging agents (42). The proapoptotic targets of the activated JNK are not clearly defined, but the phosphorylation of transcription factors such as c-Jun and p53, as well as regulation of pro- and antiapoptotic Bcl-2 family members, have been suggested to be of importance (43). In our study, JNK activation is involved in the events of IOA-mediated mitochondrial apoptotic pathway, which is completely inhibited by means of JNK1 siRNA-based inhibition, including Bax augmentation, Bcl-2 down-regulation, and apoptosis induction. These results show that the p38 pathway may operate in cell cycle arrest, and that the JNK cascade of events plays a role in apoptosis induced by IOA.

In conclusion, the present study has shown that (a) human breast cancer cells MCF-7 and MDA-MB-231 are highly sensitive to growth inhibition by IOA in both *in vitro* and *in vivo* experimental models; (b) reduced survival of either MCF-7 and MDA-MB-231 cells after exposure to IOA is associated with G₂-M phase cell cycle arrest and apoptosis induction; (c) IOA can inhibit cell cycle progression at the G₂-M phase by increasing p21 expression and by decreasing the expression of cdc2, cdc25C, cyclin B1, and cyclin A; (d) IOA-induced cell growth inhibition in the MCF-7 and MDA-MB-231 cells is mediated by the production of ROS, which activates ASK1 by decreasing the interaction of ASK1 and thioredoxin or 14-3-3, and increasing phosphorylation of ASK1 at Thr⁸⁴⁵; and (e) ASK1 activates p38 and JNK and triggers the subsequent p38-dependent cell cycle arrest and JNK-mediated apoptosis. These data provide a basic mechanism for the chemotherapeutic properties of IOA in breast cancer cells. Future *in vivo* studies using human patients may ascertain whether this cell growth inhibition effect of IOA might contribute its overall chemotherapy effects in the fight against breast cancer and its possible future therapeutic applications.

Acknowledgments

Received 3/27/2007; revised 5/8/2007; accepted 5/22/2007.

Grant support: National Science Council of Taiwan (NSC 95-2314-B-041-003).

The costs of publication of this article were defrayed in part by the payment of page charges. This article must therefore be hereby marked *advertisement* in accordance with 18 U.S.C. Section 1734 solely to indicate this fact.

We thank Professor Chun-Ching Lin (Graduate Institute of Natural Products, Kaohsiung Medical University, Kaohsiung, Taiwan) for providing nude mice and the experimental space.

References

1. Baselga J, Mendelsohn J. The epidermal growth factor receptor as a target for therapy in breast carcinoma. *Breast Cancer Res Treat* 1994;29:127-38.
2. Bange J, Zwick E, Ullrich A. Molecular targets for breast cancer therapy and prevention. *Nat Med* 2001;7:548-52.
3. Roy AM, Baliga MS, Katiyar SK. Epigallocatechin-3-gallate induces apoptosis in estrogen receptor-negative human breast carcinoma cells via modulation in protein expression of p53 and Bax and caspase-3 activation. *Mol Cancer Ther* 2005;4:81-90.
4. Bubici C, Papa S, Dean K, Franzoso G. Mutual cross-talk between reactive oxygen species and nuclear factor- κ B: molecular basis and biological significance. *Oncogene* 2006;25:6731-48.
5. Fujino G, Noguchi T, Takeda K, Ichijo H. Thioredoxin and protein kinases in redox signaling. *Semin Cancer Biol* 2006;16:427-35.
6. Kondo N, Nakamura H, Masutani H, Yodoi J. Redox regulation of human thioredoxin network. *Antioxid Redox Signal* 2006;8:1881-90.
7. Schumacker PT. Reactive oxygen species in cancer cells: live by the sword, die by the sword. *Cancer Cell* 2006;10:175-6.
8. Mounjaroen J, Nimmanit U, Callery PS, et al. Reactive oxygen species mediate caspase activation and apoptosis induced by lipoic acid in human lung epithelial cancer cells through Bcl-2 down-regulation. *J Pharmacol Exp Ther* 2006;319:1062-9.
9. Ham YM, Lim JH, Na HK, et al. Ginsenoside-Rh2-induced mitochondrial depolarization and apoptosis are associated with reactive oxygen species- and Ca^{2+} -mediated c-Jun NH₂-terminal kinase 1 activation in HeLa cells. *J Pharmacol Exp Ther* 2006;319:1276-85.
10. Kim BC, Kim HG, Lee SA, et al. Genipin-induced apoptosis in hepatoma cells is mediated by reactive oxygen species/c-Jun NH₂-terminal kinase-dependent activation of mitochondrial pathway. *Biochem Pharmacol* 2005;70:1398-407.
11. Ling YH, Liebes L, Zou Y, Perez-Soler R. Reactive oxygen species generation and mitochondrial dysfunction in the apoptotic response to bortezomib, a novel proteasome inhibitor, in human H460 non-small cell lung cancer cells. *J Biol Chem* 2003;278:33714-23.
12. Imoto K, Kukidome D, Nishikawa T, et al. Impact of mitochondrial reactive oxygen species and apoptosis signal-regulating kinase 1 on insulin signaling. *Diabetes* 2006;55:1197-204.
13. Hsieh CC, Papaconstantinou J. Thioredoxin-ASK1 complex levels regulate ROS-mediated p38 MAPK pathway activity in livers of aged and long-lived Snell dwarf mice. *FASEB J* 2006;20:259-68.
14. Nishitoh H, Matsuzawa A, Tobiume K, et al. ASK1 is essential for endoplasmic reticulum stress-induced neuronal cell death triggered by expanded polyglutamine repeats. *Genes Dev* 2002;16:1345-55.
15. Tobiume K, Matsuzawa A, Takahashi T, et al. ASK1 is required for sustained activations of JNK/p38 MAP kinases and apoptosis. *EMBO Rep* 2001;2:222-8.
16. Ouyang M, Shen X. Critical role of ASK1 in the 6-hydroxydopamine-induced apoptosis in human neuroblastoma SH-SY5Y cells. *J Neurochem* 2006;97:234-44.
17. Hwang JR, Zhang C, Patterson C. C-terminus of heat shock protein 70-interacting protein facilitates degradation of apoptosis signal-regulating kinase 1 and inhibits apoptosis signal-regulating kinase 1-dependent apoptosis. *Cell Stress Chaperones* 2005;10:147-56.
18. Matsuzawa A, Nishitoh H, Tobiume K, Takeda K, Ichijo H. Physiological roles of ASK1-mediated signal transduction in oxidative stress- and endoplasmic reticulum stress-induced apoptosis: advanced findings from ASK1 knockout mice. *Antioxid Redox Signal* 2002;4:415-25.
19. Goldman EH, Chen L, Fu H. Activation of apoptosis signal-regulating kinase 1 by reactive oxygen species through dephosphorylation at serine 967 and 14-3-3 dissociation. *J Biol Chem* 2004;279:10442-9.
20. Liu H, Zhang H, Iles KE, et al. The ADP-stimulated NADPH oxidase activates the ASK-1/MKK4/JNK pathway in alveolar macrophages. *Free Radic Res* 2006;40:865-74.
21. Song JJ, Lee YJ. Differential role of glutaredoxin and thioredoxin in metabolic oxidative stress-induced activation of apoptosis signal-regulating kinase 1. *Biochem J* 2003;373:845-53.
22. Liu H, Nishitoh H, Ichijo H, Kyriakis JM. Activation of apoptosis signal-regulating kinase 1 (ASK1) by tumor necrosis factor receptor-associated factor 2 requires prior dissociation of the ASK1 inhibitor thioredoxin. *Mol Cell Biol* 2000;20:2198-208.
23. Saitoh M, Nishitoh H, Fujii M, et al. Mammalian thioredoxin is a direct inhibitor of apoptosis signal-regulating kinase (ASK) 1. *EMBO J* 1998;17:2596-606.
24. Su JL, Lin MT, Hong CC, et al. Resveratrol induces FasL-related apoptosis through Cdc42 activation of ASK1/JNK-dependent signaling pathway in human leukemia HL-60 cells. *Carcinogenesis* 2005;26:1-10.
25. Saeki K, Kobayashi N, Inazawa Y, et al. Oxidation-triggered c-Jun N-terminal kinase (JNK) and p38 mitogen-activated protein (MAP) kinase pathways for apoptosis in human leukaemic cells stimulated by epigallocatechin-3-gallate (EGCG): a distinct pathway from those of chemically induced and receptor-mediated apoptosis. *Biochem J* 2002;368:705-20.
26. Chen CH, Lo WL, Liu YC, Chen CY. Chemical and cytotoxic constituents from the leaves of *Cinnamomum kotoense*. *J Nat Prod* 2006;69:927-33.
27. Hsu YL, Cho CY, Kuo PL, Huang YT, Lin CC. Plumbagin (5-hydroxy-2-methyl-1,4-naphthoquinone) induces apoptosis and cell cycle arrest in A549 cells through p53 accumulation via c-Jun NH₂-terminal kinase-mediated phosphorylation at serine 15 *in vitro* and *in vivo*. *J Pharmacol Exp Ther* 2006;318:484-94.
28. Freedman VH, Shin SI. Cellular tumorigenicity in nude mice: correlation with cell growth in semi-solid medium. *Cell* 1974;3:355-9.
29. Hengartner MO. The biochemistry of apoptosis. *Nature* 2000;407:770-6.
30. Valko M, Rhodes CJ, Moncol J, Izakovic M, Mazur M. Free radicals, metals and antioxidants in oxidative stress-induced cancer. *Chem Biol Interact* 2006;160:1-40.
31. Haga N, Fujita N, Tsuruo T. Involvement of mitochondrial aggregation in arsenic trioxide (As₂O₃)-induced apoptosis in human glioblastoma cells. *Cancer Sci* 2005;96:825-33.
32. Kallio A, Zheng A, Dahllund J, Heiskanen KM, Harkonen P. Role of mitochondria in tamoxifen-induced rapid death of MCF-7 breast cancer cells. *Apoptosis* 2005;10:1395-410.
33. Su YT, Chang HL, Shyue SK, Hsu SL. Emodin induces apoptosis in human lung adenocarcinoma cells through a reactive oxygen species-dependent mitochondrial signaling pathway. *Biochem Pharmacol* 2005;70:229-41.
34. Ueda S, Masutani H, Nakamura H, Tanaka T, Ueno M, Yodoi J. Redox control of cell death. *Antioxid Redox Signal* 2002;4:405-14.
35. Estrela JM, Ortega A, Obrador E. Glutathione in cancer biology and therapy. *Crit Rev Clin Lab Sci* 2006;43:143-81.
36. Kim SJ, Miyoshi Y, Taguchi T, et al. High thioredoxin expression is associated with resistance to docetaxel in primary breast cancer. *Clin Cancer Res* 2005;11:8425-30.
37. Yuan L, Yu WM, Qu CK. DNA damage-induced G₂/M checkpoint in SV40 large T antigen-immortalized embryonic fibroblast cells requires SHP-2 tyrosine phosphatase. *J Biol Chem* 2003;278:42812-20.
38. Lavelle D, DeSimone J, Hankewych M, Kousnetzova T, Chen YH. Decitabine induces cell cycle arrest at the G₁ phase via p21(WAF1) and the G₂/M phase via the p38 MAP kinase pathway. *Leuk Res* 2003;27:999-1007.
39. Kurosu T, Takahashi Y, Fukuda T, Koyama T, Miki T, Miura O. p38 MAP kinase plays a role in G₂ checkpoint activation and inhibits apoptosis of human B cell lymphoma cells treated with etoposide. *Apoptosis* 2005;10:1111-20.
40. Yuan JP, Wang GH, Ling H, et al. Diallyl disulfide-induced G₂/M arrest of human gastric cancer MGC803 cells involves activation of p38 MAP kinase pathways. *World J Gastroenterol* 2004;10:2731-4.
41. Perdiguero E, Nebreda AR. Regulation of Cdc25C activity during the meiotic G₂/M transition. *Cell Cycle* 2004;3:733-7.
42. Shen HM, Liu ZG. JNK signaling pathway is a key modulator in cell death mediated by reactive oxygen and nitrogen species. *Free Radic Biol Med* 2006;40:928-39.
43. Kim BJ, Ryu SW, Song BJ. JNK- and p38 kinase-mediated phosphorylation of Bax leads to its activation and mitochondrial translocation and to apoptosis of human hepatoma HepG2 cells. *J Biol Chem* 2006;281:21256-65.